

# Dynamical Jahn-Teller effect in the first excited $C_{60}^-$

Zhishuo Huang<sup>1, a)</sup> and Dan Liu<sup>2, 1, b)</sup>

<sup>1)</sup> *Theory of Nanomaterials Group, KU Leuven, Celestijnenlaan 200F, B-3001 Leuven, Belgium*

<sup>2)</sup> *Shaanxi Institute of Flexible Electronics, Northwestern Polytechnical University, 127 West Youyi Road, Xi'an, 710072, Shaanxi, China.*

(Dated: 18 March 2022)

The Jahn-Teller effect of  $C_{60}$  anions in the first electronically excited states was theoretically investigated. The orbital vibronic coupling parameters for the  $t_{1g}$  next lowest unoccupied molecular orbitals were derived from the Kohn-Sham orbital levels with hybrid B3LYP functional by using the frozen phonon approach. With the use of these coupling parameters, the vibronic states of the first excited  $C_{60}^-$  were derived by exactly diagonalizing the dynamical Jahn-Teller Hamiltonian. The dynamical Jahn-Teller stabilization energy of the first excited  $C_{60}^-$  is stronger than that of the ground electronic states.

## I. INTRODUCTION

Highly symmetric  $C_{60}^1$  exhibits complex Jahn-Teller (JT) dynamics characterized by orbital-vibration entanglement in various charged and excited states<sup>2-4</sup>. Negatively charged  $C_{60}$  has been one of the most investigated because it forms various molecular crystals<sup>5-11</sup>. Since the molecular nature strongly remains in these materials, for the thorough understanding of the JT effect of  $C_{60}$  anions is crucial. Though JT effect, including dynamic JT one, of  $C_{60}$  anions has been intensively investigated<sup>12-35</sup>, it is only last years that the actual situation in the ground electronic states of  $C_{60}^{n-}$  molecule ( $n = 1 - 5$ ) has been established with accurate coupling parameters<sup>33,34</sup>.

The JT effect is also considered to be important in the excited states of  $C_{60}$  anions. For example, the JT effect in the first excited  $C_{60}$  anion where the  $t_{1g}$  next lowest unoccupied molecular orbitals (NLUMOs) is populated is of fundamental importance to interpret absorption spectra of isolated  $C_{60}^-$ <sup>23,29,36-42</sup>, electron transfer process of fullerene<sup>43,44</sup>, and excitation spectra of alkali-doped fullerenes<sup>45-47</sup>. The importance is also suggested<sup>48</sup> in recently reported light induced superconductivity of alkali-doped fullerenes<sup>49,50</sup>. Moreover, the JT effect involving the NLUMO must be significant in highly alkali doped<sup>45</sup> and alkali-earth/rare-earth doped fullerenes<sup>51-57</sup>.

So far, the dynamic JT effect in negatively charged  $C_{60}$  in the ground electronic configuration where only the  $t_{1u}$  LUMOs has been mainly investigated. Recently, bound excited states of  $C_{60}^-$  have been theoretically investigated<sup>58-62</sup>, and the stability of the first excited  $^2T_{1g}$  electronic states of  $C_{60}^-$  has been confirmed. Nevertheless, the JT effect in the excited  $C_{60}$  has not been theoretically investigated, and the actual situation in  $C_{60}$  anions remains unclear.

In this work, we address the JT effect of first excited  $C_{60}^-$  anion of  $t_{1g}^1$  configuration. The vibronic coupling

parameters are derived from the  $t_{1g}$  orbital energy levels calculated by density functional theory (DFT) calculations with hybrid B3LYP exchange-correlation functional. Using these coupling parameters, the vibronic states are obtained by numerically diagonalizing the dynamical JT Hamiltonian matrix. Compared with the case of the ground electronic state of  $C_{60}^-$ ,  $t_{1u}^1$ , the stabilization in the present case is found to be stronger by about 20 %.

## II. JAHN-TELLER EFFECT

### A. Model Hamiltonian

The  $t_{1g}$  next LUMO of neutral  $C_{60}$  with  $I_h$  symmetry is triply degenerate and separated from the other orbital levels<sup>2</sup>. According to the selection rule, the  $t_{1g}$  orbitals couple to totally symmetric  $a_g$  and five-fold degenerate  $h_g$  normal modes as in the case of  $t_{1u}$  orbitals<sup>63</sup>:

$$[t_{1g} \otimes t_{1g}] = a_g \oplus h_g. \quad (1)$$

Therefore, the linear vibronic Hamiltonian of  $C_{60}^-$  in the first excited  $t_{1g}^1$  electronic configuration is given as in the case of  $t_{1u}^1$ <sup>2,12,17,64</sup>:

$$H = H_a + H_h, \quad (2)$$

$$H_a = \frac{1}{2} (p_a^2 + \omega_a^2 q_a^2) + V_a q_a, \quad (3)$$

$$H_h = \sum_{\gamma=\theta,\epsilon,\xi,\eta,\zeta} \frac{1}{2} (p_{h\gamma}^2 + \omega_h^2 q_{h\gamma}^2) + V_h \begin{pmatrix} \frac{1}{2} q_{h\theta} - \frac{\sqrt{3}}{2} q_{h\epsilon} & \frac{\sqrt{3}}{2} q_{h\zeta} & \frac{\sqrt{3}}{2} q_{h\eta} \\ \frac{\sqrt{3}}{2} q_{h\zeta} & \frac{1}{2} q_{h\theta} + \frac{\sqrt{3}}{2} q_{h\epsilon} & \frac{\sqrt{3}}{2} q_{h\xi} \\ \frac{\sqrt{3}}{2} q_{h\eta} & \frac{\sqrt{3}}{2} q_{h\xi} & -q_{h\theta} \end{pmatrix} \quad (4)$$

We take the equilibrium structure of  $C_{60}$  as the reference structure. Here,  $q_{\Gamma\gamma}$  and  $p_{\Gamma\gamma}$  ( $\gamma = \theta, \epsilon, \xi, \eta, \zeta$  for  $\Gamma = h$ ) are mass-weighted normal coordinates<sup>65</sup> and conjugate momenta, respectively,  $\omega_{\Gamma}$  is frequency, and  $V_{\Gamma}$  the vibronic coupling parameters. The basis of the matrix is in the order of  $|T_{1g}x\rangle$ ,  $|T_{1g}y\rangle$ ,  $|T_{1g}z\rangle$ .

<sup>a)</sup> zhishuohuang@gmail.com

<sup>b)</sup> iamdliu@nwpu.edu.cn

The representation for the normal coordinates and conjugate momenta possess the symmetry of real  $d$ -type  $[(2z^2 - x^2 - y^2)/\sqrt{6}, (x^2 - y^2)/\sqrt{2}, \sqrt{2}yz, \sqrt{2}zx, \sqrt{2}xy]$ , as they are consistent with the original and most used representation<sup>2,12,13,17,64</sup>. The bases are different from those ( $Q$ ) of some previous work<sup>15</sup>:

$$q_\theta = \sqrt{\frac{3}{8}}Q_\theta + \sqrt{\frac{5}{8}}Q_\epsilon, \quad q_\epsilon = \sqrt{\frac{3}{8}}Q_\theta - \sqrt{\frac{5}{8}}Q_\epsilon. \quad (5)$$

In the above equation, the indices  $g$  or  $u$  indicating the parity and the indices  $\mu$  distinguishing the frequencies are omitted for simplicity. They are added when necessary.

### B. Adiabatic potential energy surface

The model Hamiltonians, and hence the formulae, for the ground electronic configuration and the first excited configuration have the same structure. The depth of the adiabatic potential energy surface (APES) with respect to the reference structure is given by<sup>64</sup>

$$\begin{aligned} U_{\min} &= -E_a - E_{JT} \\ &= -\frac{V_a^2}{2\omega_a^2} - \frac{V_h^2}{2\omega_h^2}, \end{aligned} \quad (6)$$

with

$$q_{a,0} = -\frac{V_a}{\omega_a^2}, \quad |q_{h,0}| = \frac{V_h}{\omega_h^2}, \quad (7)$$

where  $E_a$  and  $E_{JT}$  are the first and the second terms in the last expression in Eq. (6), respectively, and  $q_h$  is the list of  $q_{h\gamma}$ . The APES has two-dimensional continuous trough<sup>64</sup>, suggesting the presence of SO(3) symmetry<sup>66,67</sup>.

### C. Vibronic states

As in the case of the JT problem for the  $t_{1u}^1$  configurations<sup>66-68</sup>, the vibronic angular momenta  $\hat{J}$  exist in the case of  $t_{1g}^1$ :

$$[\hat{H}_h, \hat{J}^2] = [\hat{H}_h, \hat{J}_z] = 0. \quad (8)$$

Therefore, the eigenstates of  $\hat{H}$  (vibronic states) are expressed by  $J$ ,  $M_J$ , and principal quantum number  $\alpha$ ,

$$\hat{H}_h|\alpha JM_J\rangle = E_{\alpha J}|\alpha JM_J\rangle. \quad (9)$$

The analytical treatments of the vibronic states in the strong limit of vibronic coupling<sup>12,17,32,64,66</sup> and weak coupling limit<sup>13</sup> have been discussed much. Nevertheless, for the quantitative description of C<sub>60</sub> ions, only numerical approach can provide accurate description.

For numerical calculations, it is convenient to expand the vibronic states as

$$|\alpha JM_J\rangle = \sum_{\gamma} \sum_{\mathbf{n}_h} |T_{1g}\gamma\rangle \otimes |\mathbf{n}\rangle C_{\gamma\mathbf{n};\alpha JM_J}. \quad (10)$$

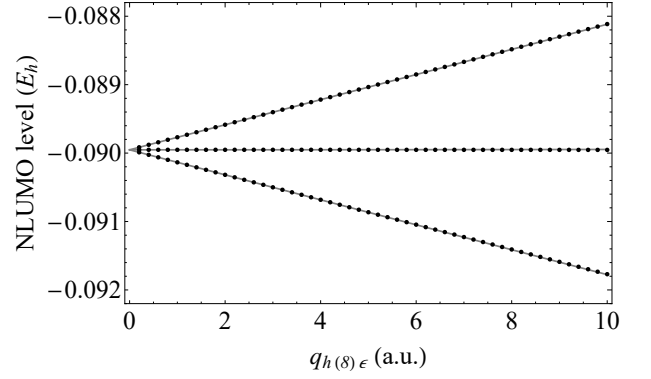


FIG. 1. The JT splitting of the NLUMO levels with respect to  $q_{h(8)\epsilon}$  deformation (in atomic unit). The black points and gray lines indicate the DFT values and model energy, respectively.

Here,  $\mathbf{n}_h = (n_{h\theta}, n_{h\epsilon}, n_{h\xi}, n_{h\eta}, n_{h\zeta})$  is the set of vibrational quantum numbers of the Harmonic oscillation part of Eq. (4). Such an expansion using the direct products of the electronic states and the eigenstates of harmonic oscillator has been proposed long time ago<sup>69</sup> and has been routinely used as a reliable approach to quantitatively study the dynamical JT systems including fullerene anions<sup>12,16,17,26,30,33,66,70</sup>.

In the present calculations, the vibrational basis is truncated as

$$0 \leq n_{h(\mu)\gamma}, \quad \sum_{\mu\gamma} n_{h(\mu)\gamma} \leq 7, \quad (11)$$

because the dimension of the Hamiltonian matrix rapidly increases. To take account of the eight sets of  $h_g$  modes in real C<sub>60</sub>,  $\mu$  is shown. For the diagonalization of the vibronic Hamiltonian (4), Lanczos algorithm was employed<sup>71</sup>.

### D. Orbital vibronic coupling parameters

The orbital vibronic coupling parameters are defined by the gradients of the  $t_{1g}$  NLUMO level:

$$v_a = \left. \frac{\partial \epsilon_{t_{1g}z}}{\partial q_a} \right|_{\mathbf{q}=0}, \quad v_h = - \left. \frac{\partial \epsilon_{t_{1g}z}}{\partial q_{h\theta}} \right|_{\mathbf{q}=0}, \quad (12)$$

where  $\mathbf{q}$  is the set of all normal coordinates. In the present case, the vibronic coupling parameters  $V_\Gamma$  correspond to the orbital vibronic coupling parameters  $v_\Gamma$ :

$$V_\Gamma = v_\Gamma, \quad (13)$$

in a good approximation because of the very small mixing of the orbitals under JT deformation.

The vibronic coupling parameters are derived by fitting the model potential to the gradients of NLUMO levels of neutral C<sub>60</sub> calculated in Ref. 34. The derivations were done using the DFT data with hybrid B3LYP functional because in the studies of C<sub>60</sub> anions, this functional

TABLE I. The frequencies  $\omega_\Gamma$  ( $\text{cm}^{-1}$ ), vibronic coupling parameters  $V_\Gamma$  ( $10^{-4}$  a.u.), dimensionless vibronic coupling parameters  $g_\Gamma = V_\Gamma/\sqrt{\hbar\omega_\Gamma^3}$ , and stabilization energies  $E_\Gamma$  (meV) for the  $a_g$  and  $h_g$  modes. The data for LUMO are taken from Ref.<sup>34</sup> and the frequencies are taken from Ref.<sup>72</sup>.

$J$			NLUMO			LUMO		
$\Gamma$	$\mu$	$\omega_\Gamma$	$V_\Gamma$	$g_\Gamma$	$E_\Gamma$	$V_\Gamma$	$g_\Gamma$	$E_\Gamma$
$a_g$	1	496	-0.449	-0.418	5.38	-0.264	-0.245	1.849
	2	1470	-2.480	-0.452	18.66	-2.380	-0.422	16.543
$h_g$	1	273	-0.406	-0.926	14.50	0.192	0.455	3.415
	2	437	-0.476	-0.536	7.78	0.450	0.503	6.886
	3	710	-1.061	-0.577	14.64	0.754	0.396	7.069
	4	774	-0.594	-0.284	3.86	0.554	0.259	3.256
	5	1099	-0.498	-0.141	1.35	0.766	0.209	3.038
	6	1250	-1.664	-0.387	11.61	0.578	0.132	1.360
	7	1428	0.125	0.024	0.05	2.099	0.394	13.867
	8	1575	-2.113	-0.348	11.79	2.043	0.326	10.592

has been shown to give the coupling parameters close to those derived from experimental data<sup>26</sup> [In the study, high-resolution photoelectron spectra<sup>73</sup> was used]. The coupling parameters derived from the B3LYP data are in good agreement with those from the gradients of the GW quasiparticle levels<sup>74</sup>. Furthermore, with the use of these parameters, the spin gap of  $C_{60}^{3-}$  was well reproduced<sup>33</sup>. The vibronic coupling parameters of  $C_{60}^-$  have been derived using local density approximation<sup>75</sup>, generalized gradient approximation<sup>25</sup>, and also by post Hartree-Fock calculations<sup>76</sup>. Nevertheless, the former two methods underestimate and the latter one overestimates the vibronic coupling parameters. Therefore, we expect that the vibronic coupling parameters derived from the gradient of the NLUMO levels are accurate enough to reveal the low-energy states of excited  $C_{60}^-$ .

The derived vibronic coupling parameters are listed in Table I and one of the fittings is shown in Fig. 1 (see for the other fittings Supplemental Materials). In the fitting, the  $h_g\epsilon$  deformation is used instead of the  $h_g\theta$  with  $v_h = -(2/\sqrt{3})\partial\epsilon_x/\partial q_{h\epsilon}|_{q=0}$ . The stabilization energies (6) in the  $T_{1g}$  electronic states are  $E_a = 24.0$  and  $E_h = 65.6$  meV, which are by 30.7 % and 32.5 % larger than the stabilization energies of for the  $a_g$  and  $h_g$  modes in the  $T_{1u}$  ground electronic states, respectively.

### E. Vibronic states

The vibronic Hamiltonian matrix was numerically diagonalized as described in Sec. II C. The calculated data are listed in Table II and the levels are shown in Fig. 2. In the figure, the vibronic levels for the ground  $C_{60}^-$  and the vibrational levels of neutral  $C_{60}$  as well as the vibronic levels of the first excited  $C_{60}^-$ . The ground vibronic and vibrational levels are used as the origin of the energy.

One should note that the distributions of the vibronic states of  $C_{60}$  anions differ much from that of the vibra-

tional levels of neutral  $C_{60}$ . The ground vibronic levels with vibronic angular momentum  $J=1$  for the  $T_{1u}$  ( $t_{1u}^1$ ) and  $T_{1g}$  ( $t_{1g}^1$ ) electronic states are -96.5 and -113.8 meV, respectively. Previous study shows that for the ground electronic states, the contributions from the static and the dynamic JT effect to the ground energy are almost the same<sup>33</sup>. However, the ratio of the dynamical contribution to the static contribution is smaller in the  $t_{1g}^1$  case than in the  $t_{1u}^1$  case (Table III), which is consistent<sup>12,17</sup> with the stronger orbital vibronic couplings for the  $t_{1g}$  NLUMO than for the  $t_{1u}$  LUMO.

The difference in the vibronic couplings in the  $t_{1u}$  and the  $t_{1g}$  levels appear in the excited vibronic levels too (Fig. 2). The group of the first excited vibronic levels ( $J = 3, 2, 1$ ) split more in the case of  $t_{1g}^1$  than in  $t_{1u}^1$ , as expected from the stronger vibronic coupling in the former: the splitting of the former, 13.3 meV, is about two times larger than that of LUMO (4.4 meV). Such splitting may be observed as fine structures in e.g. high-resolution absorption spectra of  $C_{60}^-$ .

### III. DISCUSSION

The dynamical JT effect in the  $T_{1g}$  electronic states has been discussed in e.g. Refs. 23 and 39. Indeed, as found in Sec. II E, the stabilization by the dynamical JT effect is even stronger than in the ground electronic states (Table III), suggesting the importance of the vibronic dynamics in the excited electronic states.

The presence of the dynamical JT effect in the excited states can be found in various spectroscopic data. For example, one should note that the signs of almost all the vibronic coupling parameters for the  $h_g$  modes in the  $T_{1g}$  state, and hence the JT deformations, are opposite to those for the  $T_{1u}$  state. The difference in the direction of the JT deformations in the  $T_{1u}$  and the  $T_{1g}$  states indicate that the relative displacements in these electronic states are large, and thus, the vibronic progression in the

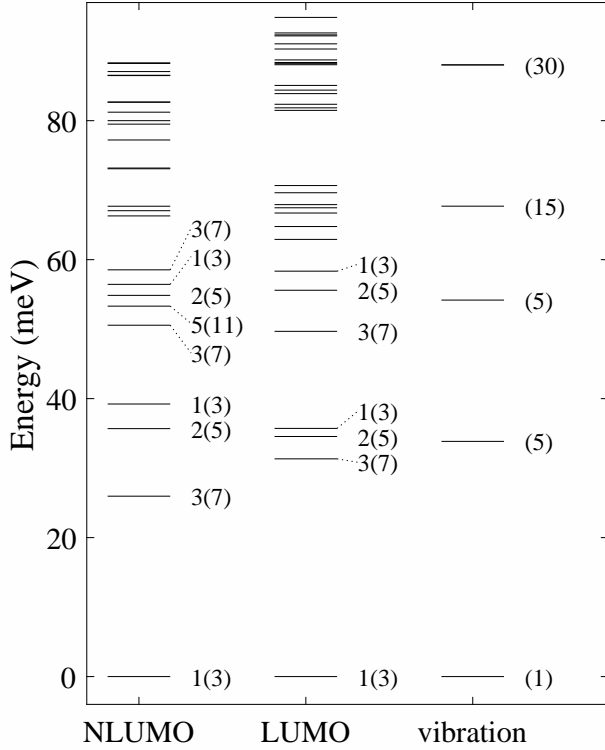


FIG. 2. Low-lying vibronic levels with respect to the first excited states, the ground states and zero-vibrational level of  $C_{60}^-$ . The numbers next to the energy levels are  $J$  with the degeneracy shown in the parenthesis.

excitation spectra of  ${}^2T_{1g} \leftarrow {}^2T_{1u}$  tends to be stronger than that in the photoelectron spectra of  $C_{60}^-$  because the latter is only related to the vibronic coupling in the  $T_{1u}$  state. Indeed, the peaks in the absorption spectra of  $C_{60}^-$ <sup>23,39</sup> are stronger than the peaks in the photoelectron spectra of  $C_{60}^-$ <sup>73,77</sup>. Furthermore, as mentioned in Sec. II E, the transition to the excited vibronic states may be seen as the fine structure of the spectra.

By combining the present vibronic coupling parameters for the  $t_{1g}$  NLUMO with those for the  $t_{1u}$  LUMO (Table I), it is also possible to address diverse problems of  $C_{60}$ . For example, the  $(T_{1u} \oplus T_{1g}) \otimes h_g$  product Jahn-Teller problem<sup>78</sup> in  $C_{60}^{2-}$  anion  $t_{1u}^1 t_{1g}^1$  electron configurations. Since the signs of the orbital vibronic coupling parameters for the  $t_{1u}$  and the  $t_{1g}$  levels tend to be opposite to each other, the resulting vibronic coupling of the first excited  $C_{60}^{2-}$  must be weak. Besides, the combination of the present vibronic coupling constants and those for  $C_{60}^+$ <sup>79</sup> enables us to investigate the luminescence spectra<sup>80</sup> involving  $t_{1g}$  NLUMO.

#### IV. CONCLUSION

In this work, the vibronic coupling parameters of the  $T_{1g}$  electronic states of  $C_{60}^-$  by using the next lowest unoccupied molecular orbital levels at B3LYP level. Based

TABLE II. The vibronic energy levels with respect to the first excited states and the ground states of  $C_{60}^-$  (meV). The data for are taken Ref.<sup>34</sup>, and the number in the parentheses indicate  $J$ .

$J$		NLUMO	LUMO
1	1	-113.815	-96.469
	2	-74.589	-60.753
	3	-57.370	-38.126
	4	-47.520	-29.757
	5	-40.736	-26.841
	6	-31.168	-11.395
	7	-25.493	-8.099
	8	-	-5.411
	9	-	-4.123
2	1	-78.132	-61.918
	2	-58.955	-40.873
	3	-46.127	-29.004
	4	-31.122	-12.071
	5	-26.748	-8.264
	6	-	-6.155
	7	-	-4.265
3	1	-87.854	-65.135
	2	-63.252	-46.786
	3	-55.282	-31.703
	4	-40.633	-25.806
	5	-33.815	-14.620
	6	-32.593	-12.575
	7	-25.581	-8.417
	8	-	-3.843
	9	-	-1.607
4	1	-46.772	-28.549
	2	-34.314	-14.108
	3	-27.326	-7.724
5	1	-60.505	-33.554
	2	-36.593	-14.985
	3	-27.281	-

TABLE III. Contributions to the ground vibronic energy ( $E_{total}$ ) of NLUMO and LUMO of  $C_{60}^-$ .  $E_{static}$ , and  $E_{dynamic}$  represent the static JT and dynamic JT stabilization energies. Ratio refers the ratio between  $E_{static}$  and  $E_{dynamic}$  ( $E_{dynamic}/E_{static}$ ).

Orbital	$E_{total}$	$E_{static}$	$E_{dynamic}$	Ratio
NLUMO	-113.8	-65.6	-48.2	0.74
LUMO <sup>33</sup>	-96.46	-50.3	-46.2	0.92

on the obtained parameters, the vibronic states were calculated by exactly diagonalizing the dynamical Jahn-Teller Hamiltonian. The results for the  $t_{1g}^1$  configuration showed stronger dynamic JT stabilization than that for the  $t_{1u}^-$  configuration by about 20 %, indicating the importance of the JT effect in the excited states. The pres-



ence of the JT dynamics appears in spectroscopic data. Due to the difference in the direction of the JT deformations in the  $T_{1u}$  and the  $T_{1g}$  states, stronger vibronic progression is seen in the absorption spectra than in the photoelectron spectra of  $C_{60}^-$ .

## ACKNOWLEDGMENTS

The authors thank Naoya Iwahara and Liviu Chibotaru for fruitful discussions. They also gratefully acknowledge funding by the China Scholarship Council (CSC).

- <sup>1</sup>H. W. Kroto, J. R. Heath, S. C. O'Brien, R. F. Curl, and R. E. Smalley, " $C_{60}$ : Buckminsterfullerene," *Nature* **318**, 162–163 (1985).
- <sup>2</sup>C. C. Chancey and M. C. M. O'Brien, *The Jahn-Teller Effect in  $C_{60}$  and Other Icosahedral Complexes* (Princeton University Press, Princeton, 1997).
- <sup>3</sup>I. B. Bersuker, *The Jahn-Teller Effect* (Cambridge University Press, Cambridge, 2006).
- <sup>4</sup>J. L. Dunn, H. S. Alqannas, and A. J. Lakin, "Jahn-Teller effects and surface interactions in multiply-charged fullerene anions and the effect on scanning tunneling microscopy images," *Chem. Phys.* **460**, 14 (2015).
- <sup>5</sup>O. Gunnarsson, *Alkali-Doped Fullerenes: Narrow-Band Solids with Unusual Properties* (World Scientific, Singapore, 2004).
- <sup>6</sup>M. Capone, M. Fabrizio, C. Castellani, and E. Tosatti, "Colloquium: Modeling the unconventional superconducting properties of expanded  $a3c60$  fullerides," *Reviews of Modern Physics* **81**, 943 (2009).
- <sup>7</sup>Alloul, H., "Electronic correlations, jahn-teller distortions and mott transition to superconductivity in alkali- $c60$  compounds," *EPJ Web of Conferences* **23**, 00015 (2012).
- <sup>8</sup>K. Kamarás and G. Klupp, "Metallicity in fullerides," *Dalton Transactions* **43**, 7366–7378 (2014).
- <sup>9</sup>Y. Takabayashi and K. Prassides, "Unconventional high- $T_c$  superconductivity in fullerides," *Philosophical Transactions of the Royal Society A: Mathematical, Physical and Engineering Sciences* **374**, 20150320 (2016).
- <sup>10</sup>Y. Nomura, S. Sakai, M. Capone, and R. Arita, "Exotic  $s$ -wave superconductivity in alkali-doped fullerides," *J. Phys. Condens. Matter* **28**, 153001 (2016).
- <sup>11</sup>A. Otsuka, D. V. Konarev, R. N. Lyubovskaya, S. S. Khasanov, M. Maesato, Y. Yoshida, and G. Saito, "Design of spin-frustrated monomer-type  $c60$  mott insulator," *Crystals* **8** (2018), 10.3390/cryst8030115.
- <sup>12</sup>A. Auerbach, N. Manini, and E. Tosatti, "Electron-vibron interactions in charged fullerenes. I. Berry phases," *Phys. Rev. B* **49**, 12998 (1994).
- <sup>13</sup>N. Manini, E. Tosatti, and A. Auerbach, "Electron-vibron interactions in charged fullerenes. II. Pair energies and spectra," *Phys. Rev. B* **49**, 13008 (1994).
- <sup>14</sup>W.-Z. Wang, A. R. Bishop, and L. Yu, "Dynamic jahn-teller-induced infrared absorption of a charged  $c_{60}^-$  molecule," *Phys. Rev. B* **50**, 5016–5019 (1994).
- <sup>15</sup>J. L. Dunn and C. A. Bates, "Analysis of the  $T_{1u} \otimes h_g$  Jahn-Teller system as a model for  $C_{60}$  molecules," *Phys. Rev. B* **52**, 5996 (1995).
- <sup>16</sup>O. Gunnarsson, H. Handschuh, P. S. Bechthold, B. Kessler, G. Ganteför, and W. Eberhardt, "Photoemission Spectra of  $C_{60}^-$ : Electron-Phonon Coupling, Jahn-Teller Effect, and Superconductivity in the Fullerides," *Phys. Rev. Lett.* **74**, 1875 (1995).
- <sup>17</sup>M. C. M. O'Brien, "Vibronic energies in  $C_{60}^{n-}$  and the Jahn-Teller effect," *Phys. Rev. B* **53**, 3775 (1996).
- <sup>18</sup>E. Tosatti, N. Manini, and O. Gunnarsson, "Surprises in the orbital magnetic moment and  $g$  factor of the dynamic jahn-teller ion  $c_{60}^-$ ," *Phys. Rev. B* **54**, 17184–17190 (1996).
- <sup>19</sup>W. Wang, C. Wang, A. Bishop, L. Yu, and Z. Su, "Dynamic jahn-teller effect in fullerene  $c60$  and related observable effects," *Synthetic Metals* **86**, 2365 – 2368 (1997), proceedings of the International Conference on Science and Technology of Synthetic Metals.
- <sup>20</sup>N. Manini and E. Tosatti, "Exact zero-point energy shift in the  $e \otimes (nE)$ ,  $t \otimes (nH)$  many-modes dynamic jahn-teller systems at strong coupling," *Phys. Rev. B* **58**, 782–790 (1998).
- <sup>21</sup>S. Sookhun, J. L. Dunn, and C. A. Bates, "Jahn-Teller effects in the fullerene anion  $C_{60}^{2-}$ ," *Phys. Rev. B* **68**, 235403 (2003).
- <sup>22</sup>J. L. Dunn and H. Li, "Jahn-Teller effects in the fullerene anion  $C_{60}^{3-}$ ," *Phys. Rev. B* **71**, 115411 (2005).
- <sup>23</sup>S. Tomita, J. U. Andersen, E. Bonderup, P. Hvelplund, B. Liu, S. B. Nielsen, U. V. Pedersen, J. Rangama, K. Hansen, and O. Echt, "Dynamic Jahn-Teller Effects in Isolated  $C_{60}^-$  Studied by Near-Infrared Spectroscopy in a Storage Ring," *Phys. Rev. Lett.* **94**, 053002 (2005).
- <sup>24</sup>I. D. Hands, J. L. Dunn, C. A. Bates, M. J. Hope, S. R. Meech, and D. L. Andrews, "Vibronic interactions in the visible and near-infrared spectra of  $C_{60}^-$  anions," *Phys. Rev. B* **77**, 115445 (2008).
- <sup>25</sup>T. Frederiksen, K. J. Franke, A. Arnau, G. Schulze, J. I. Pascual, and N. Lorente, "Dynamic Jahn-Teller effect in electronic transport through single  $C_{60}$  molecules," *Phys. Rev. B* **78**, 233401 (2008).
- <sup>26</sup>N. Iwahara, T. Sato, K. Tanaka, and L. F. Chibotaru, "Vibronic coupling in  $C_{60}^-$  anion revisited: Derivations from photoelectron spectra and DFT calculations," *Phys. Rev. B* **82**, 245409 (2010).
- <sup>27</sup>J. L. Dunn, A. J. Lakin, and I. D. Hands, "Manifestation of dynamic jahn-teller distortions and surface interactions in scanning tunnelling microscopy images of the fullerene anion  $c-60$ ," *New Journal of Physics* **14**, 083038 (2012).
- <sup>28</sup>G. Klupp, P. Matus, K. Kamarás, A. Y. Ganin, A. McLennan, M. J. Rosseinsky, Y. Takabayashi, M. T. McDonald, and K. Prassides, "Dynamic Jahn-Teller effect in the parent insulating state of the molecular superconductor  $Cs_3C_{60}$ ," *Nat. Commun.* **3**, 912 (2012).
- <sup>29</sup>K. Stöckel and J. U. Andersen, "Photo excitation and laser detachment of  $C_{60}^-$  anions in a storage ring," *J. Chem. Phys.* **139**, 164304 (2013).
- <sup>30</sup>P. Ponzellini, *Computation of the paramagnetic  $g$ -factor for the fullerene monocation and monoanion*, Master's thesis, Milan University (2014).
- <sup>31</sup>K. Kundu, D. R. Kattnig, B. Mladenova, G. Grampp, and R. Das, "Electron Spin Relaxation of  $C_{60}$  Monoanion in Liquid Solution: Applicability of Kivelson-Orbach Mechanism," *J. Phys. Chem. A* **119**, 3200 (2015).
- <sup>32</sup>N. Iwahara, "Berry phase of adiabatic electronic configurations in fullerene anions," *Phys. Rev. B* **97**, 075413 (2018).
- <sup>33</sup>D. Liu, N. Iwahara, and L. F. Chibotaru, "Dynamical jahn-teller effect of fullerene anions," *Phys. Rev. B* **97**, 115412 (2018).
- <sup>34</sup>D. Liu, Y. Niwa, N. Iwahara, T. Sato, and L. F. Chibotaru, "Quadratic Jahn-Teller effect of fullerene anions," *Phys. Rev. B* **98**, 035402 (2018).
- <sup>35</sup>Y. Matsuda, N. Iwahara, K. Tanigaki, and L. F. Chibotaru, "Manifestation of vibronic dynamics in infrared spectra of mott insulating fullerides," *Phys. Rev. B* **98**, 165410 (2018).
- <sup>36</sup>T. Kato, T. Kodama, T. Shida, T. Nakagawa, Y. Matsui, S. Suzuki, H. Shiromaru, K. Yamauchi, and Y. Achiba, "Electronic absorption spectra of the radical anions and cations of fullerenes:  $C_{60}$  and  $C_{70}$ ," *Chemical Physics Letters* **180**, 446 – 450 (1991).
- <sup>37</sup>T. Kato, T. Kodama, and T. Shida, "Spectroscopic studies of the radical anion of  $C_{60}$ . Detection of the fluorescence and reinvestigation of the ESR spectrum," *Chem. Phys. Lett.* **205**, 405 (1993).
- <sup>38</sup>T. Kodama, T. Kato, T. Moriwaki, H. Shiromaru, and Y. Achiba, "Laser study on the resonance-enhanced multipho-

- ton electron detachment (ramped) processes for c60- and c70-," *The Journal of Physical Chemistry* **98**, 10671–10673 (1994).
- <sup>39</sup>H. Kondo, T. Momose, and T. Shida, "Reinvestigation of the low-lying electronic states of  $C_{60}^-$ ," *Chem. Phys. Lett.* **237**, 111 (1995).
- <sup>40</sup>O.-H. Kwon, H. Yoo, K. Park, B. Tu, R. Ryoo, and D.-J. Jang, "Anionic and upper-excited fluorescence of c60 encapsulated in  $\gamma$  zeolitic nanocavity," *The Journal of Physical Chemistry B* **105**, 4195–4199 (2001).
- <sup>41</sup>O.-H. Kwon, H. Yoo, and D.-J. Jang, "Photophysics of c60 and c60-in faujasite zeolites," *The European Physical Journal D - Atomic, Molecular, Optical and Plasma Physics* **18**, 69 (2002).
- <sup>42</sup>S. Watariguchi, M. Fujimori, K. Atsumi, and T. Hinoue, "Evidences of electron transfer of a fullerene anion radical (c60-) prepared under visible-light illumination at a nitrobenzene/water interface," *Analytical Sciences* **32**, 463–468 (2016).
- <sup>43</sup>M. Fujitsuka, C. Luo, and O. Ito, "Electron-transfer reactions between fullerenes (c60 and c70) and tetrakis(dimethylamino)ethylene in the ground and excited states," *The Journal of Physical Chemistry B* **103**, 445–449 (1999).
- <sup>44</sup>M. Fujitsuka, T. Ohsaka, and T. Majima, "Dual electron transfer pathways from the excited c60 radical anion: enhanced reactivities due to the photoexcitation of reaction intermediates," *Phys. Chem. Chem. Phys.* **17**, 31030–31038 (2015).
- <sup>45</sup>M. Knupfer and J. Fink, "Mott-hubbard-like behavior of the energy gap of  $a_4C_{60}$  ( $a = \text{na, k, rb, cs}$ ) and  $\text{na}_{10}C_{60}$ ," *Phys. Rev. Lett.* **79**, 2714–2717 (1997).
- <sup>46</sup>L. F. Chibotaru and A. Ceulemans, "Symmetry breaking and the band structure of fullerides: the concomitant role of jahn-teller interactions and electron correlation," in *Proc. XIV Int. Symp. on Electron-Phonon Dynamics and Jahn-Teller Effect* (World Scientific, 1999) pp. 233–240.
- <sup>47</sup>L. F. Chibotaru and A. Ceulemans, "Broken-symmetry band structure description of the spectroscopy of  $k_3c_{60}$ ," *AIP Conference Proceedings* **544**, 19–23 (2000).
- <sup>48</sup>A. Nava, C. Giannetti, A. Georges, E. Tosatti, and M. Fabrizio, "Cooling quasiparticles in  $A_3C_{60}$  fullerides by excitonic mid-infrared absorption," *Nat. Phys.* **14**, 154 (2018).
- <sup>49</sup>M. Mitrano, A. Cantaluppi, D. Nicoletti, S. Kaiser, A. Perucchi, S. Lupi, P. D. Pietro, D. Pontiroli, M. Ricc , S. R. Clark, D. Jaksch, and A. Cavalleri, "Possible light-induced superconductivity in  $K_3C_{60}$  at high temperature," *Nature* **530**, 461 (2016).
- <sup>50</sup>A. Cantaluppi, M. Buzzi, G. Jotzu, D. Nicoletti, M. Mitrano, D. Pontiroli, M. Ricc , A. Perucchi, P. D. Pietro, and A. Cavalleri, "Pressure tuning of light-induced superconductivity in  $K_3C_{60}$ ," *Nat. Phys.* **14**, 837 (2018).
- <sup>51</sup>X. H. Chen, S. Taga, and Y. Iwasa, "Raman-scattering study of ba-doped  $c_{60}$  with  $t_{1g}$  states," *Phys. Rev. B* **60**, 4351–4356 (1999).
- <sup>52</sup>S. Margadonna, E. Aslanis, W. Z. Li, K. Prassides, A. N. Fitch, and T. C. Hansen, "Crystal structure of superconducting  $k_3ba_3c_{60}$ : a combined synchrotron x-ray and neutron diffraction study," *Chemistry of Materials* **12**, 2736–2740 (2000).
- <sup>53</sup>Y. Iwasa and T. Takenobu, "Superconductivity, mott hubbard states, and molecular orbital order in intercalated fullerides," *Journal of Physics: Condensed Matter* **15**, R495–R519 (2003).
- <sup>54</sup>H. Li, S. He, H. Zhang, B. Lu, S. Bao, H. Li, P. He, Y. Xu, and T. Hao, "Electronic structure of  $yb_{2.75}c_{60}$ ," *Phys. Rev. B* **68**, 165417 (2003).
- <sup>55</sup>S.-L. He, H.-N. Li, X.-X. Wang, H.-Y. Li, Y.-B. Xu, S.-N. Bao, K. Ibrahim, H.-J. Qian, R. Su, J. Zhong, C.-H. Hong, and M. I. Abbas, "Synchrotron radiation photoemission study of Yb-intercalated  $c_{60}$ ," *Phys. Rev. B* **71**, 085404 (2005).
- <sup>56</sup>M. Akada, T. Hirai, J. Takeuchi, T. Yamamoto, R. Kumashiro, and K. Tanigaki, "Superconducting phase sequence in  $R_xc_{60}$  fullerides ( $r = \text{Sm and yb}$ )," *Phys. Rev. B* **73**, 094509 (2006).
- <sup>57</sup>S. Heguri and M. Kobayashi, "Magnetic susceptibility of magnesium fulleride  $mg_4c_{60}$ ," *Chemical Physics Letters* **490**, 34 – 37 (2010).
- <sup>58</sup>S. Klaiman, E. V. Gromov, and L. S. Cederbaum, "Extreme correlation effects in the elusive bound spectrum of c60," *The Journal of Physical Chemistry Letters* **4**, 3319–3324 (2013).
- <sup>59</sup>S. Klaiman, E. V. Gromov, and L. S. Cederbaum, "All for one and one for all: accommodating an extra electron in c60," *Phys. Chem. Chem. Phys.* **16**, 13287–13293 (2014).
- <sup>60</sup>V. G. Zakrzewski, O. Dolgounitcheva, and J. V. Ortiz, "Electron propagator calculations on the ground and excited states of c60," *The Journal of Physical Chemistry A* **118**, 7424–7429 (2014).
- <sup>61</sup>E. V. Gromov, S. Klaiman, and L. S. Cederbaum, "Influence of ligand field on the ground and excited superatomic and valence states of c60," *Molecular Physics* **113**, 2964–2969 (2015).
- <sup>62</sup>E. V. Gromov, S. Klaiman, and L. S. Cederbaum, "How many bound valence states does the c60 anion have?" *Phys. Chem. Chem. Phys.* **18**, 10840–10845 (2016).
- <sup>63</sup>H. A. Jahn and E. Teller, "Stability of Polyatomic Molecules in Degenerate Electronic States. I. Orbital Degeneracy," *Proc. R. Soc. Lond. A* **161**, 220 (1937).
- <sup>64</sup>M. C. M. O'Brien, "Dynamic Jahn-Teller Effect in an Orbital Triplet State Coupled to Both  $E_g$  and  $T_{2g}$  Vibrations," *Phys. Rev.* **187**, 407 (1969).
- <sup>65</sup>T. Inui, Y. Tanabe, and Y. Onodera, *Group Theory and Its Applications in Physics* (Springer-Verlag, Berlin and Heidelberg, 1990).
- <sup>66</sup>M. C. M. O'Brien, "The jahn-teller effect in a p state equally coupled to eg and t2g vibrations," *Journal of Physics C: Solid State Physics* **4**, 2524–2536 (1971).
- <sup>67</sup>D. R. Pooler, "Continuous group invariances of linear Jahn-Teller systems. II. Extension and application to icosahedral systems," *J. Phys. C: Solid St. Phys.* **13**, 1029 (1980).
- <sup>68</sup>R. Romestain and Y. Merle d'Aubign , "Jahn-Teller Effect of an Orbital Triplet Coupled to Both  $E_g$  and  $T_{2g}$  Modes of Vibrations: Symmetry of the Vibronic States," *Phys. Rev. B* **4**, 4611 (1971).
- <sup>69</sup>H. C. Longuet-Higgins, U.  pik, M. H. L. Pryce, and R. A. Sack, "Studies of the jahn-teller effect .ii. the dynamical problem," *Proceedings of the Royal Society of London. Series A. Mathematical and Physical Sciences* **339**, 1–13 (1975).
- <sup>70</sup>N. Iwahara and L. F. Chibotaru, "Dynamical Jahn-Teller Effect and Antiferromagnetism in  $Cs_3C_{60}$ ," *Phys. Rev. Lett.* **111**, 056401 (2013).
- <sup>71</sup>D. R. Pooler, "Numerical diagonalization techniques in the jahn-teller effect," in *The Dynamical Jahn-Teller Effect in Localized Systems*, edited by Y. E. Perlin and M. Wagner (Elsevier, Amsterdam, 1984) Chap. 6, p. 199.
- <sup>72</sup>D. S. Bethune, G. Meijer, W. C. Tang, H. J. Rosen, W. G. Golden, H. Seki, C. A. Brown, and M. S. de Vries, "Vibrational raman and infrared spectra of chromatographically separated c60 and c70 fullerene clusters," *Chemical Physics Letters* **179**, 181 – 186 (1991).
- <sup>73</sup>X.-B. Wang, H.-K. Woo, and L.-S. Wang, "Vibrational cooling in a cold ion trap: vibrationally resolved photoelectron spectroscopy of cold  $C_{60}^-$  anions," *J. Chem. Phys.* **123**, 051106 (2005).
- <sup>74</sup>C. Faber, J. L. Janssen, M. C  t , E. Runge, and X. Blase, "Electron-phonon coupling in the  $C_{60}$  fullerene within the many-body GW approach," *Phys. Rev. B* **84**, 155104 (2011).
- <sup>75</sup>N. Manini, A. D. Corso, M. Fabrizio, and E. Tosatti, "Electron-vibration coupling constants in positively charged fullerene," *Philosophical Magazine B* **81**, 793–812 (2001).
- <sup>76</sup>N. Iwahara, T. Sato, K. Tanaka, and L. F. Chibotaru, "Estimation of the vibronic coupling constants of fullerene monoanion: Comparison between experimental and simulated results," in *Vibronic Interactions and the Jahn-Teller Effect: Theory and Applications*, edited by M. Atanasov, C. Daul, and P. L. Tregenna-Piggott (Springer Netherlands, Dordrecht, 2012) pp. 245–264.
- <sup>77</sup>D.-L. Huang, P.-D. Dau, H.-T. Liu, and L.-S. Wang, "High-resolution photoelectron imaging of cold  $C_{60}^-$  anions and accurate determination of the electron affinity of  $C_{60}$ ," *J. Chem. Phys.* **140**, 224315 (2014).

- <sup>78</sup>A. Ceulemans and L. F. Chibotaru, “Icosahedral  $t_{1u}+t_{1g}$  jahn-teller problem,” Phys. Rev. B **53**, 2460–2462 (1996).
- <sup>79</sup>Z. Huang and D. Liu, “First principles study of the vibronic coupling in positively charged  $c_{60}^+$ ,” arXiv preprint arXiv:1905.00530 (2019).
- <sup>80</sup>I. Akimoto and K.-i. Kan’no, “Photoluminescence and Near-Edge Optical Absorption in the Low-Temperature Phase of Pristine  $C_{60}$  Single Crystals,” Journal of the Physical Society of Japan **71**, 630–643 (2002).

# Supplement Material: Dynamical Jahn-Teller effect in the first excited $C_{60}^-$

Zhishuo Huang<sup>1, a)</sup> and Dan Liu<sup>2, 1, b)</sup>

<sup>1)</sup> *Theory of Nanomaterials Group, KU Leuven, Celestijnenlaan 200F, B-3001 Leuven, Belgium*

<sup>2)</sup> *Shaanxi Institute of Flexible Electronics, Northwestern Polytechnical University, 127 West Youyi Road, Xi'an, 710072, Shaanxi, China*

(Dated: 18 March 2022)

Supplemental Materials contain the JT splitting of the NLUMO levels with respect to  $q_{h\epsilon}$  deformation.

## I. JT SPLITTING OF THE NLUMO LEVELS

There are eight  $q_{h\epsilon}$  deformation, which are distinguished by the subindex, as  $q_{h(1)\epsilon}$  corresponding to the first  $q_{h\epsilon}$  deformation. The splitting pattern of the NLUMO levels with respect to  $q_{h(i)\epsilon}$  ( $i=1,2,\dots,8$ ) deformation are shown in Fig. 1, 2, 3, 4, 5, 6, 7, and 8, respectively.

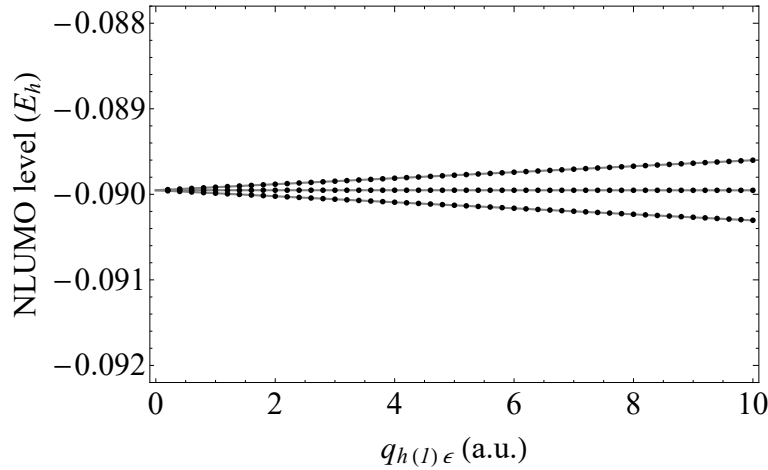


FIG. 1. The JT splitting of the NLUMO levels with respect to  $q_{h_g(1)\epsilon}$  deformation (in atomic unit). The black points and gray lines indicate the DFT values and model energy, respectively.

<sup>a)</sup>Electronic mail: zhishuohuang@gmail.com

<sup>b)</sup>Electronic mail: iamdliu@nwpu.edu.cn



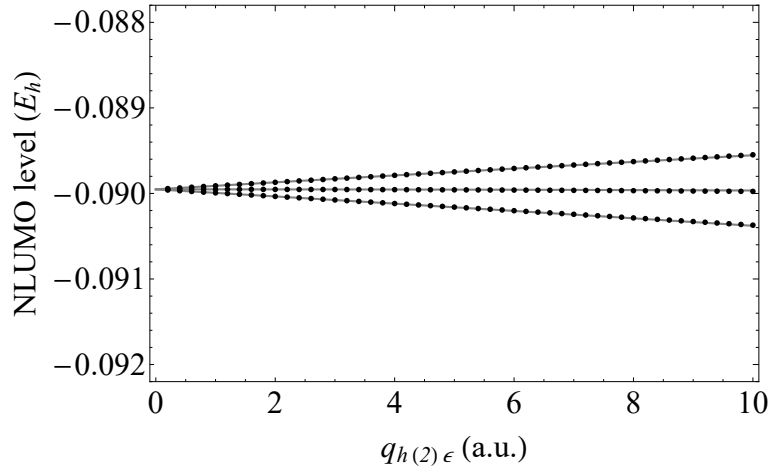


FIG. 2. The JT splitting of the NLUMO levels with respect to  $q_{hg(2)}\epsilon$  deformation (in atomic unit). The black points and gray lines indicate the DFT values and model energy, respectively.

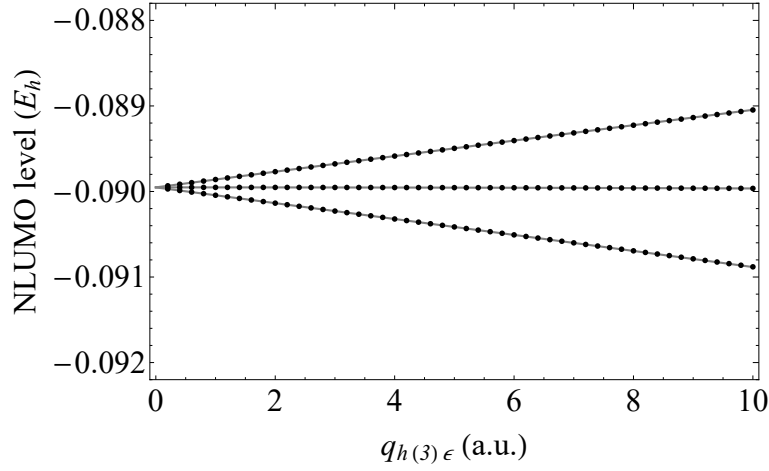


FIG. 3. The JT splitting of the NLUMO levels with respect to  $q_{hg(3)}\epsilon$  deformation (in atomic unit). The black points and gray lines indicate the DFT values and model energy, respectively.

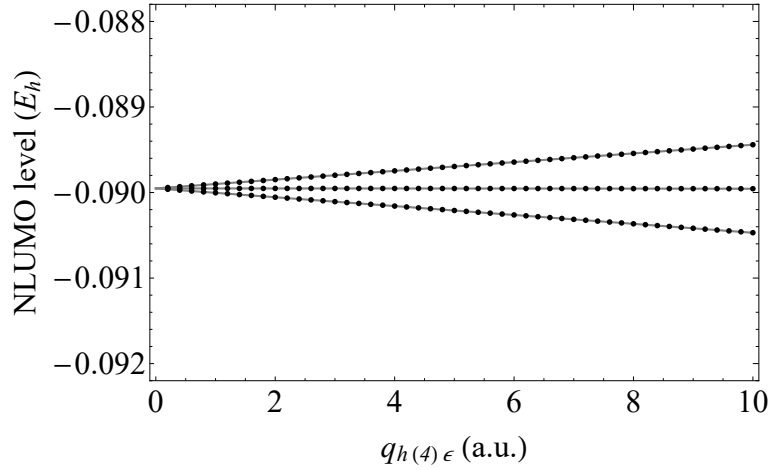


FIG. 4. The JT splitting of the NLUMO levels with respect to  $q_{hg(4)}\epsilon$  deformation (in atomic unit). The black points and gray lines indicate the DFT values and model energy, respectively.

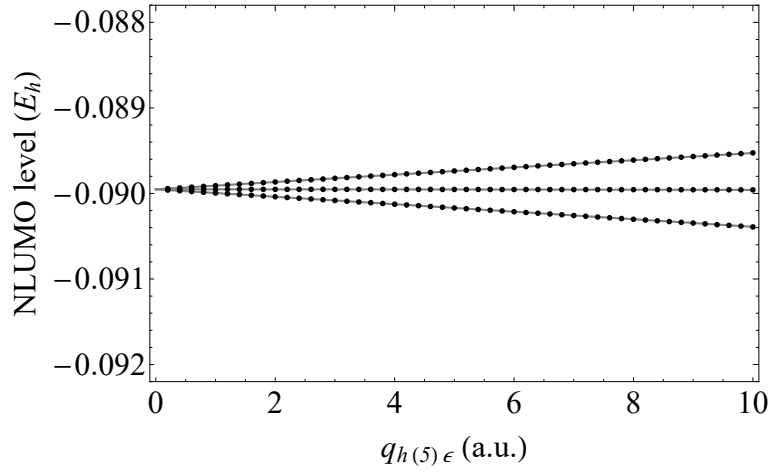


FIG. 5. The JT splitting of the NLUMO levels with respect to  $q_{hg(5)}\epsilon$  deformation (in atomic unit). The black points and gray lines indicate the DFT values and model energy, respectively.

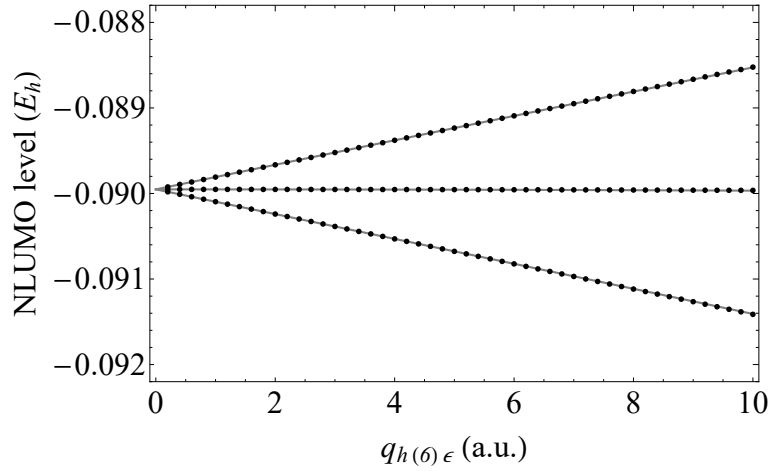


FIG. 6. The JT splitting of the NLUMO levels with respect to  $q_{hg(6)}\epsilon$  deformation (in atomic unit). The black points and gray lines indicate the DFT values and model energy, respectively.

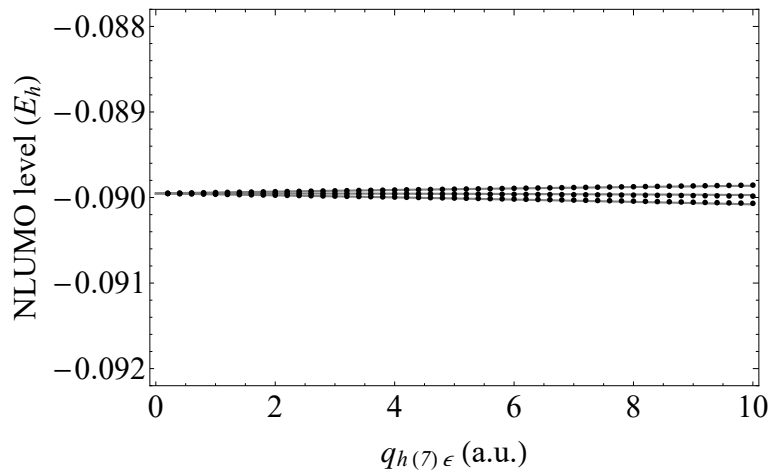


FIG. 7. The JT splitting of the NLUMO levels with respect to  $q_{hg(7)}\epsilon$  deformation (in atomic unit). The black points and gray lines indicate the DFT values and model energy, respectively.

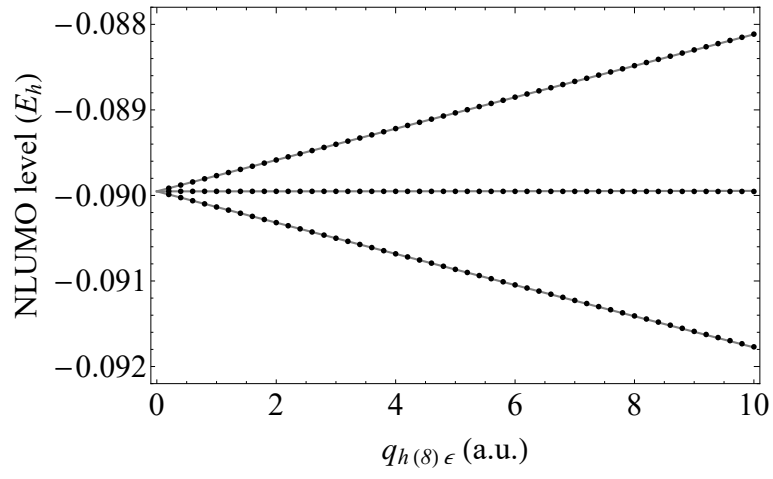


FIG. 8. The JT splitting of the NLUMO levels with respect to  $q_{h_g(s)}\epsilon$  deformation (in atomic unit). The black points and gray lines indicate the DFT values and model energy, respectively.